Received: 13 January 2018 | Accepted: 16 November 2018

DOI: 10.1002/jcb.28246

RESEARCH ARTICLE

WILEY Journal of Cellular Biochemistry

Nrf2 dependent antiaging effect of milk-derived bioactive peptide in old fibroblasts

Naveen Kumar MSc, PhD Scholar[1] | Srinu Reddi PhD[1] | Savita Devi MSc, PhD[1] | Sanusi Bello Mada PhD[1,2] | Rajeev Kapila PhD[1] | Suman Kapila PhD[1]

[1]Animal Biochemistry Division, ICAR-National Dairy Research Institute, Karnal, India

[2]Department of Biochemistry, Ahmadu Bello University, Zaria, Nigeria

Correspondence
Suman Kapila, PhD, Animal Biochemistry Division, ICAR-National Dairy Research Institute, Karnal 132001, India.
Email: skapila69@gmail.com

Funding information
ICAR-National Dairy Research Institute; CSIR-UGC-MHRD

Abstract

Prolonged passaging of primary fibroblast cells totally shapes the natural biological phenomena and leads to the appearance of features related to senescence. As a result, it is a good natural tool to delineate the molecular mechanism of cellular aging. The present investigation revealed the antiaging effect of milk-derived novel bioactive peptide (VLPVPQK). The peptide played an important role in downregulating apoptosis-related markers in late passages of cultured fibroblast cells. The peptide treatment to aged fibroblasts caused enhancement in cell migration, DNA integrity, and decrease in the lipid peroxidation, reactive oxygen species, nitric oxide production as well as pro-inflammatory cytokines, TNF-α and IL-6. Moreover, the peptide decreased the expression of apoptotic caspases, Bax, and senescence-associated β-galactosidase (SA-β-gal) proteins. The peptide pretreatment also enhanced the extracellular collagen protein and anti-apoptotic, Bcl-xL. In addition, the peptide treatment reversed the senescence-related activity in fibroblasts by stimulating Nrf2 mediated antioxidative defense system and inhibiting the action of NFkB/p38MAPK signaling, similar to the commercially available inhibitor (SB203580) of p38MAPK. Thus, the peptide exhibits the antiaging effect in dermal fibroblast cells.

Highlights

1. A novel bioactive peptide, VLPVPQK shows antiaging effect in prolonged serial passaged fibroblast cells.
2. The peptide causes activation and transmigration of Nrf2 for maintaining homeostasis.
3. The peptide rejuvenates the aged fibroblast cells by weakening the effects of the senescent associated secretory phenotype.

Abbreviations: AKT, protein kinase B; DCFH-DA, 2′7′-dichlorofluorescin diacetate; DMEM, Dulbecco modified Eagle's medium; DMSO, dimethyl sulfoxide; EP, early passage; ERK, Extracellular-signal-regulated kinase; FBS, fetal bovine serum; FITC, fluorescein isothiocyanate; LP, late passage; MAPK, mitogen-activated protein kinases; MTT, thiazolyl blue tetrazolium bromide; NO, Nitric oxide; Nrf2, nuclear factor-E2-related factor 2; PBS, phosphate buffered saline; Pep, VLPVPQK; ROS, reactive oxygen species; X-gal, 5-bromo-4-chloro-3-indolyl-β-D-galactopyranoside.

4. The peptide alleviates the NF-kB/p38MAP kinase pathway in aged fibroblasts.

KEYWORDS
bioactive peptide, p38MAP kinase, prolonged serial passage, senescence-associated secretory phenotype

1 | INTRODUCTION

Cells in vitro reveal limited proliferative potential before entering a state of irreversible growth arrest in which cells remain metabolically active and mitotically inactive, called as cellular aging or replicative senescence.[1-3] Fibroblasts, a main cell type of skin, contribute majorly to the collagen synthesis and connective tissue homeostasis. Consequently, fibroblasts malfunctioning leads to aging as demonstrated by many histological studies.[4-7] In addition, cell synchronization can be achieved by exposing cells to low serum conditions in vitro.[8] Thus, culturing fibroblast cells in low serum conditions till late passages (natural aging) offer the best model for screening the regulation of molecular mechanism by antiaging compounds in vitro. Secondly, this senescent cell growth arrest through p38 pathway occurs via regulation by global cyclin-dependent kinase inhibitor, p21. Thus, it reduces cell spreading and increases ROS production and consequently, downregulates the collagen synthesis due to impaired transforming growth factor beta signaling.[4-7,9,10] Besides this, the cellular redox imbalance by ROS reduces cell viability through stimulating proapoptotic caspases.[11-13] It is the phosphorylation and subsequent, nuclear transport of transcription factors such as nuclear factor-E2-related factor 2 (Nrf2), induces ARE-mediated gene expression of superoxide dismutase (SOD), catalase (CAT), glutathione (GSH) that protect cells against damage.[14] In the present era of health hazardous molecules, harmless low doses of natural compounds like bioactive peptides are gaining immense importance. These molecules stimulate an adaptive stress response by impacting cellular signaling mechanisms.

Apart from naturally planned complete food, milk carries incredible antioxidative, anticancer, anti-inflammatory, antihypertensive, antimicrobial, and osteogenic properties, accredited to the obscured bioactive peptides.[15-20] Recently, four novel peptides from buffalo milk casein have been isolated, purified, and sequenced by RP-HPLC and LC-MS/MS in our laboratory. Amongst four peptides, one peptide (VLPVPQK) obtained from pepsin-trypsin hydrolysates of β-casein demonstrated ACE-inhibitory, antioxidative, osteoanabolic properties and, was also bio-accessible up to 1% as earlier reported by transepithelial transport studies in Caco-2 cells.[17,21,22] But, so far no study has yet been conducted related to antiaging role of this heptapeptide. Therefore, in the present study, an attempt has been made to examine the complex signaling circuitries coupling p38 mitogen-activated protein kinases (MAPK) pathway and multiple antioxidative and antiapoptotic proteins, responsible for antiaging potential of the peptide.

2 | MATERIAL AND METHODS

Anti-Vimentin, CD86, Nrf2, NFkB (P65), P38α, p-P38α, Bcl-xL, Bax, and β-Actin antibody were purchased from Santa Cruz Biotechnology, Paso Robles, CA and Pierce Thermo Fisher Scientific, Waltham, MA. Fetal Bovine Serum (FBS) was purchased from HyClone. Casein-derived peptide, VLPVPQK (Pep) was custom synthesized (Link Biotech, New Delhi, India) and used in the present study. Nitric oxide (NO), SOD, CAT, GSH, and MDA assay kits were procured from Cayman Chemical Company, Ann Arbor, MI. Inhibitors of protein kinase B (Akt) (LY294006), extracellular-signal-regulated kinase (ERK) (U0260), and p38MAPK (SB203580), Dulbecco's modified eagle medium (DMEM), antibiotics viz. Penicillin, Streptomycin, Amphotericin-B, 2′,7′-dichlorofluorescein diacetate (DCFH-DA) dye, caspase-3 and 9 substrates, Sirius Red dye, dimethyl sulfoxide (DMSO), thiazolyl blue tetrazolium bromide (MTT) dye, and secondary antibody were purchased from Sigma-Aldrich Chemical Co, St. Louis, MO. All other reagents used in the present study were of analytical grade. The other plastic wares were purchased from Tarsons Products Pvt Ltd, (Kolkata, India); Axygen, Inc (New Delhi, India); and Millipore Pvt Ltd, Bedford, MA.

2.1 | Rat fibroblast cell isolation and culture

Rat pups (3 days old) were procured from the small animal house after taking approval from the Institutional Animal Ethics Committee. Skin fibroblast cells were isolated from 3-days old rat pup skin as described earlier[23] and cultured in T-25 cm^2 flasks in a humidified incubator at 37°C and 5% CO_2 with a cell density of 1×10^5 cells per mL of medium in each flask.

2.2 | Immunocytochemical characterization

Fibroblast cells were characterized using cytoskeleton antibodies, anti-vimentin (dilution 1:250) as a positive marker and CD 86 (dilution 1:150) as a negative marker at 5th, 10th, 20th, and 32th passage as described previously.[24] Images were examined under an epifluorescent microscope (Olympus Bx51, Shinjuku, Tokyo, Japan) and merged using Image J software.

2.3 | Experimental design and treatment protocol

Cells were sub-cultured after 70% to 80% confluency and seeded at 1:3 split ratio in DMEM containing 10% FBS. Cell viability was assessed routinely by either trypan blue exclusion or MTT.[25] In further experiments, cells were grown in only DMEM medium for 4 hours followed by treatment with DMEM media supplemented with 2% FBS containing different concentrations of peptide (5, 10, 20, 30, 50, 100, 500, and 1000 ng/mL) and without peptide as a control for 48 hours. After assessing the concentration of peptide that causes proliferation of fibroblasts, all the experiments were performed at every 5th (early passage [EP]) and 32nd (late passage [LP]) passage. Curcumin was used as positive control in this study as it has been studied extensively for its antioxidative, anti-inflammatory, and antiaging properties.[26,27]

2.4 | Proliferation assay

Fibroblast cell proliferation was assessed at both passages using the MTT[25] method. In total, 3×10^4 cells were plated in a 96-well plate. After 24 hours, cells were treated with peptide (30 and 100 ng/mL) and curcumin (15 μM) in medium containing 2% FBS for 48 hours. The absorbance was measured at 540 nm using a dual wavelength measuring system (BioTek enzyme-linked immunosorbent assay [ELISA] reader).

2.5 | Measurement of intracellular fluorescence by DCFH-DA staining

Intracellular reactive oxygen species (ROS) were determined using DCFH-DA dye following manufacturer's instructions. In brief, cells at both passages were cultured in 96-well plate at the density of 3×10^4 cells per well and cultured overnight for attachment. After overnight attachment, cells were washed with phosphate buffered saline (PBS) and incubated with or without peptide (30 ng/mL) and curcumin (15 μM) for 24 hours. After treatment, media was discarded and cells were incubated with 100 μL of DCFH-DA (50 μM) for 30 minutes in the incubator at 37°C in 5% CO_2. Then, cells were replaced with PBS and analyzed under a fluorescent microscope (Olympus). DCFH-DA fluorescence intensity was quantified using fluorescent multimode (TECAN, Infinite M200 PRO) ELISA reader at 485 nm excitation and 535 nm emission filter.

2.6 | Measurement of nitric oxide and MDA production in the cellular system

Assays were performed at both passages. Nitric oxide (NO) and MDA production was determined by cell-based assay kit (Cayman, #10009419 and #10009055, Ann Arbor, MI, respectively) following manufacturer's instructions. For NO assay, cells were treated as described in Section 2.5 and results were analyzed under fluorescent multi-plate ELISA reader at excitation and emission wavelength of 485 and 535 nm, respectively. Images were analyzed under a fluorescent microscope (Olympus) with a blue filter. Moreover, MDA detection was based on the formation of MDA-TBA adduct at high temperature and under acidic conditions. Cells were cultured in a six-well plate at a density of 3×10^5cells per well and treated with or without peptide and curcumin (15 μM) for 24 hours. After completion of treatment, adduct was measured at 530 nm.

2.7 | Measurement of DNA damage and cell apoptosis

DNA damage was examined by Hoechst 33258 proliferation assay, while cell apoptosis was measured by caspase-9/3 apoptosis assay.

2.7.1 | Hoechst 33258 proliferation assay

Cell proliferation was determined using Hoechst 33258 as described previously.[14] At both passages, cells were treated with the peptide as described in Section 2.5. After 24 hours incubation, cells were washed with PBS and stained with Hoechst 33258 (5 μg/mL in PBS) for 5 minutes. An increase in fluorescence was quantified under the fluorescent multi-plate ELISA reader with a test wavelength of 485 nm excitation and 525 nm emission filters. Images were taken randomly under a fluorescent microscope (Olympus) with UV filter.

2.7.2 | Caspase-9 and -3 apoptosis assay

Caspase-9/-3 apoptotic assays were performed at both passages and activity of both caspases were determined as described previously.[21] Cells were treated with or without peptide and curcumin. Ten microlitre each of Ac-DEVD-pNA (2 mM) and Ac-LEHD-pNA (2 mM) substrates were

used for detection of caspase-9/-3 respectively, at room temperature for 30 minutes. Released pNA was then measured at 405 nm.

2.8 | Assessment of antioxidative status

Cellular antioxidative enzymes such as SOD, CAT, and nonenzymatic activity such as reduced GSH were determined at both early (P5) and LP (P32+) by Cayman chemical assay kit (Ann Arbor) according to manufacturer's instructions. Cells were cultured in a six-well plate at the density of 3×10^5 cells per well and treated with or without peptide and curcumin (15 μM) for 24 hours. Cells were washed with PBS after treatment and scraped with a rubber policeman for protein isolation.

2.9 | Evaluation of wound healing and anti-inflammatory property

2.9.1 | Cell scratch assay

For studying the effect of the peptide on the regulation of cell migration or proliferation wound healing assay was performed in cultured fibroblast cells. The assay was performed at the LP as described earlier with some modification.[28] Briefly, cells (3×10^5 cells) were cultured into the six-well plate for 24 hours in complete growth medium till confluency and scratches were made with the p200 uL pipette tip. To obtain the same scratch areas at different time intervals, reference points were made with an ultrafine tip marker on the outer bottom of the dish were made. This was followed by washing and culturing plate in DMEM medium only for 4 hours. Then, cells were treated with or without peptide and curcumin (15 μM) for 48 hours and cell migration was monitored at 0, 24, and 48 hours. All the images were taken under an inverted microscope (Olympus 510).

2.9.2 | Estimation of pro-inflammatory cytokines

Cytokines, TNF-α, and IL-6 levels were measured using ELISA kits (Leinco Technologies, Inc, Fenton, MO; Ray Biotech, Norcross, GA, respectively) following manufacturer's instructions. Cells were grown in the six-well plate for 24 hours and treated with or without peptide and curcumin for 24 hours. After completion of treatment, the cell supernatant was collected and cytokines were estimated.

2.10 | Sircol collagen assay

For the assessment of fibrillar hue and spatial distribution of extracellular matrix (ECM), collagen content was quantified by Sirius red dye.[29] Cells were cultured in six-well plates and treated with or without peptide and curcumin for 24 hours.

2.11 | Senescence-associated β-galactosidase assay

Senescence-associated β-galactosidase (SA-β-gal) activity was measured using 5-bromo-4-chloro-3-indolyl-β-D-galactopyranoside cytochemical assay as described previously.[30] Cells were cultured and grown in six-well plates for 24 hours. Cells were treated with or without peptide and curcumin for 24 hours as described in Section 2.5. Then, the plate was stained with SA-β-gal staining solution. Images were taken under an inverted bright field microscope (Olympus 510) for the qualitative detection of SA-β-gal activity.

2.12 | Quantitative real-time polymerase chain reaction for aging markers

Cells at LP were treated with or without peptide and curcumin as described in the previous section. Total RNA was isolated by single-step RNA isolation method using Tri-reagent (Sigma-Aldrich) following manufacturer's instructions and cDNA was synthesized using the "Revert Aid first strand cDNA synthesis kit" (Thermo Fisher). Reverse transcription was performed in three steps: 5 minutes at 65°C, 55 minutes at 42°C, and 5 minutes at 70°C. Quantitative real-time polymerase chain reaction (PCR) was performed using ABI PRISM 7500 Fast detection system (Applied Biosystems, Foster City, CA) with SYBR Green (2X, Thermo Fisher Scientific). The thermal profile included incubation at 95°C for 10 minutes, followed by 40 cycles with denaturation at 95°C for 15 seconds, an annealing of 59.4°C for 45 seconds and extension. The primers used in the present study are listed in Table 1. A reaction volume consisted of 5-μL SYBR green, 3-μL diluted cDNA (5 ng), and 1 μl of each primer (10 pmol). Relative gene expressions were calculated using the $\Delta\Delta C_t$ method and normalization of expression was done with GAPDH.

2.13 | Delineation of the downstream signaling

In total, 3×10^4 cells in 100 μL media were seeded in a 96-well plate. After 24 hours, cells were treated with DMEM (2% FBS) containing inhibitors for Akt (LY294006), ERK (U0260), and P38 MAPK (SB203580), and also, supplemented with peptide (30 ng/mL) or without peptide (as control) for 24 hours. Thereafter,

TABLE 1 The sequence of primers for real-time PCR are listed as follows

Sr. no.	Gene	Accession no.	Forward primer (5′-3′)	Reverse primer (5′-3′)	Size
1	P21	XM_008763355.2	AACAGTAGACACGAAACAGGC	GCATCGTCAACACCCTGTC	96
2	P16	NM_031550.1	ACCCCGATACAGGTGATGATG	CAGAGTGTCTAGGAAGCCCTC	144
3	GAPDH	NM017008	GACAACTTTGGCATCGTGGA	ATGCAGGGATGATGTTCTGG	133

Abbreviation: PCR, polymerase chain reaction.

the medium was discarded and replaced with DMEM supplemented with 2% FBS for next 24 hours. Following this, 20 μL of MTT solution (5 mg/mL) was added to each well and the plate was incubated for 4 hours at 37°C. The formazan crystals were dissolved by adding 100 μL DMSO per well. The absorbance was measured at 540 nm using a dual wavelength measuring system (BioTek ELISA reader).

2.13.1 | Immunolocalization of phospho-p38 MAPK and Nrf2

At LP, 1×10^4 cells were seeded in a 24 well plate for 24 hours. Then, cells were treated with peptide and, co-treated with peptide and p38 MAPK inhibitor (SB203580; 20 μM) for 24 hours. At the end of the experiment, cells were fixed with ice cold methanol (15 minutes). After this, methanol was removed and PBST (PBS + 0.25% Triton-X 100) was added for permeabilization (10 minutes) at room temperature. After 10 minutes, PBST was removed by washing with PBS. After washing, the plate was blocked with a blocking solution (5% bovine serum albumin [BSA] + PBST) for 30 minutes. The blocking solution was removed and incubated with primary antibody against Nrf2 and phospho-p38 MAPK (1:500; C-20: SC-722; SC-17852, Santa Cruz Biotechnology) overnight. After incubation with primary antibody, cells were washed with PBS three times (each for 5 minutes). The secondary antibody (fluorescein isothiocyanate labeled) was added and incubated for 90 minutes in the dark condition on a shaker at room temperature. After 90 minutes, cells were washed with PBS three times (each for 10 minutes). Then, the nucleus was stained with DAPI. Images were examined under a fluorescent microscope (Olympus Bx51) and merged using image J software.

2.13.2 | Western blot analysis

After treatment of cells with peptide, cytoplasmic and nuclear proteins were isolated using protein extraction reagent (Boster, Rockford, IL) containing phosphatase inhibitors (20 mM of sodium fluoride, 1 mM of sodium orthovanadate) and protease inhibitor cocktail (Sigma) as per manufacturer's instructions. The cell lysate was centrifuged at 20 800*g* for 15 minutes and the supernatant was collected for protein quantification.[31] Then, proteins (50 μg) were resolved in 12% SDS-PAGE and transferred to PVDF membranes (Millipore Corp). After blocking with 5% nonfat dry milk (dissolved in TBST [20 mM TrisHCl (pH 7.9), 8.5% NaCl and 0.1% Tween 20]) at RT for 1 hour, the membrane was exposed to primary antibodies for anti-p38α MAPK, antiphospho p38MAPK, anti-Nrf2, anti-NFkB (P65), anti-Bax, anti-Bcl-$_X$L (1:1000; C-20: SC-535, SC-17852, SC-722, SC-372, SC-943, SC-7195, Santa Cruz Biotechnology), and anti-β-Actin (1:10000; RB-9421-P, Thermo Fisher Scientific) in TBST containing 1.0% BSA at 4°C overnight. At the end of incubation, washing was done with TBST followed by incubation with secondary horseradish peroxidase-conjugated antirabbit IgG antibody (Sigma) for 1 hour at RT. The membrane was rinsed with washing buffer (10 mM Tris-HCl [pH 9.5], 10 mM NaCl, and 1 mM $MgCl_2$), visualized with HRP reagent (Millipore Corp) and exposed to X-ray film.

3 | STATISTICAL ANALYSIS

Results were expressed as mean ± standard error of the mean (n = 3, independent experiments were performed) using GraphPad Prism 5.01 version (Graph Pad Software Inc, San Diego, CA). Comparisons were made using one and two-way ANOVA (Bonferroni post hoc test) was used to test the significance of the difference between the groups and *P* value less than 0.05 was considered as statistically significant.

4 | RESULTS

4.1 | Characterization of cultured cells

Dermal in-vitro cultured cells at different passages reflected elongated and spindle-shaped morphology of fibroblasts. Cells at early and late passages (5th, 10th, 20th, and 32th passage) were characterized by immunocytochemistry and were found to be positive for vimentin (a cytoskeletal protein and a marker for fibroblast cell identification),

whereas, no expression of CD86, a negative marker for fibroblast cells was observed (Figure 1A-i to v). The nucleus was stained blue with DAPI (10 μg/mL). These findings suggested that cell populations were certainly viable and mesodermal fibroblasts in origin.

4.2 | Proliferation of fibroblasts

To determine the effect of different concentration of peptide (5, 10, 20, 30, 50, 100, 500, and 1000 ng/mL) on cell viability was studied by MTT assay. The peptide at

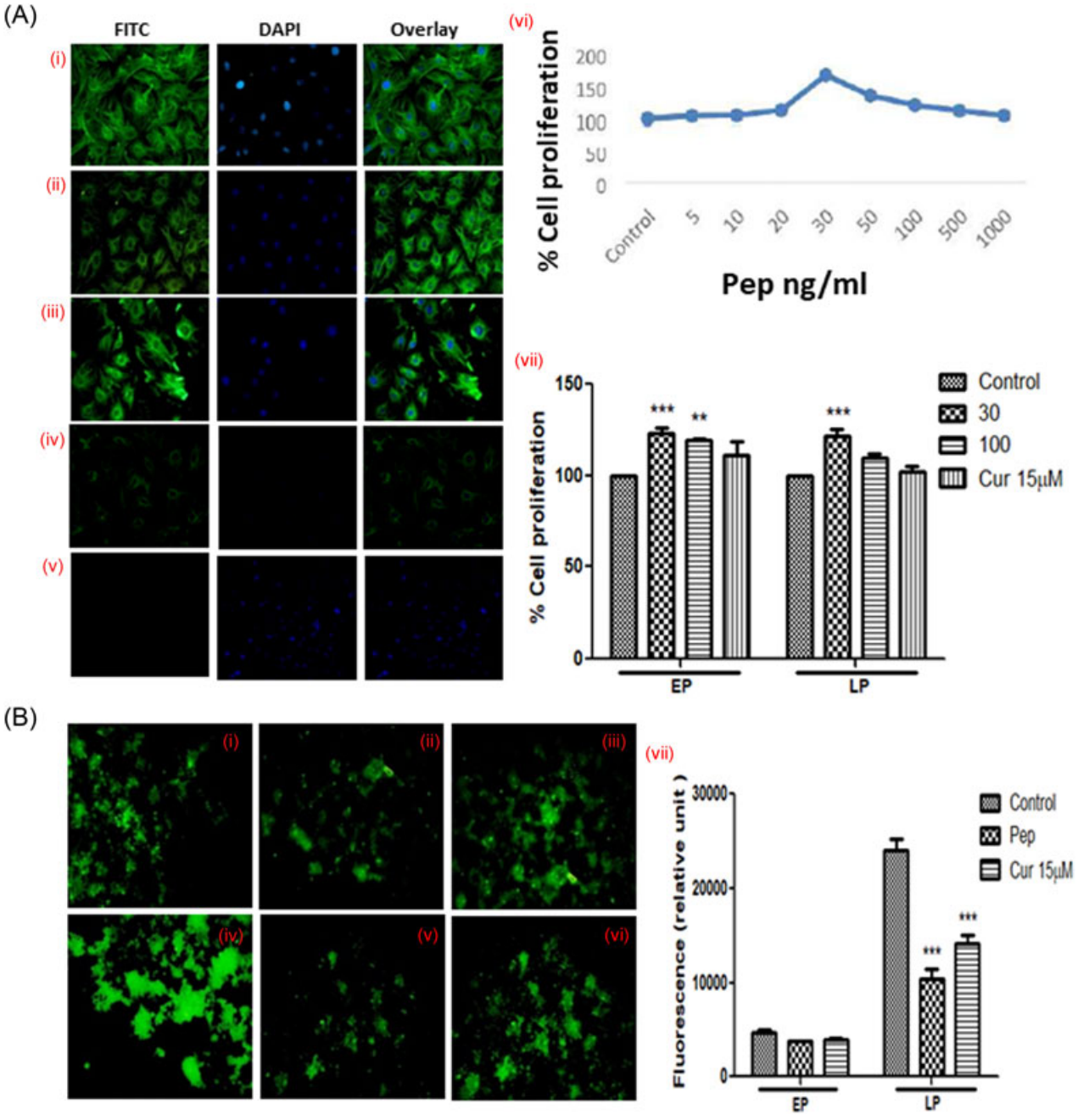

FIGURE 1 A, Immunocytochemical characterization of fibroblast cells. (i) fibroblast cells at 5th passage (ii) cells at 10th passage. (iii) Cells at 20th passage. (iv) Cells at 32nd passage with positive marker. (v) Cells negatively stained with CD86 marker. (vi) Effect of different concentration of peptide on cell proliferation (5-1000ng/ml). (vii) Proliferation of fibroblast cells at early (5th) and late (32nd) passage. n = 3, independent experiments were performed. B, Effect of the peptide on the ROS production in fibroblast cells at early passage (EP) and at late passage (LP) by DCFH-DA. Representative fluorescent images at early passage and at late passage (i) Control (ii) Peptide (iii) Curcumin 15 μM. (iv) Control (v) Peptide (vi) Curcumin 15 μM (vii) Quantitative analysis of ROS production at early and late passages. The results are expressed as mean ± SEM value for n = 3, independent experiments. $^{*}P < 0.05$, $^{**}P < 0.01$, and $^{***}P < 0.001$ in comparison to control

30 ng/mL (Pep) concentration was found to be more effective as compared to the control group at both early and late passage (Figure 1A-vi and vii).

4.3 | Measurement of oxidative stress biomarkers

4.3.1 | Shield to ROS and other related reactive molecules NO

The effect of heptapeptide on intracellular ROS and NO production was measured at both early and late passage. Pep (30 ng/mL) significantly ($P < 0.05$) reduced the ROS (Figure 1B-vii) and NO production at both passages (Figure 2A-i to vii) as compared to the control fibroblast cells. These results were also clear from fluorescent microscope studies (Figure 1B-i to vi and Figure 2A-i to vi).

4.3.2 | Inhibition of lipid peroxidation activity

A significant ($P < 0.05$) reduction in MDA level was observed in the presence of peptide and curcumin at the early and late passages (Figure 2A-viii) in comparison to the control.

4.4 | Cytoprotective effects against DNA damage and apoptosis

4.4.1 | Peptide recovers DNA damage in aged fibroblasts

Nuclear stain, Hoechst 33258 was used to detect characteristic changes in nuclear morphology. In the peptide-treated group (Figure 2B-ii and v), cells were healthy with round dividing nucleus and nuclear material was intact without condensation and fragmentation at both early (Figure 2B-ii) and late passages (Figure 2B-v) as shown in magnified images. Expanded and degraded nucleus was observed in the control group, a typical feature of apoptosis/senescence (Figure 2B-i [EP]; Figure 2B-iv [LP]). Moreover, cell proliferation rate was also significantly ($P < 0.05$) more in the peptide-treated group at both early and late passages as compared to the control as shown in Figure 2B-vii.

4.4.2 | Suppression of caspases' activity

At both the passages, the initiator caspase, that is, caspase-9 activity (Figure 2B-viii) was found to be increased, followed by an increment in executioner caspase, that is, caspase-3 activity (Figure 2B-ix) in the control; whereas peptide treatment effectively reversed the cell apoptosis, and significantly decreased ($P < 0.05$) the activities of caspases at both the passages.

4.5 | Stabilization of antioxidative system in aged cells

To further ensure the antiaging effect of the peptide, intracellular GSH level, CAT, and SOD activities were measured. The results showed that the heptapeptide treatment caused enhancement in SOD (Figure 3A-i) and catalase (Figure 3A-ii) activity only in LP, while total GSH level (Figure 3C) increased significantly ($P < 0.05$) at both the passages as compared to the control.

4.6 | Wound closure and collagen deposition by heptapeptide

4.6.1 | In-vitro fibroblast cells spreading and reduction of pro-inflammatory cytokines

The peptide treatment reduced the denudation of the cellular area at a faster rate. Because it induced cell proliferation and migration from all sides of the scratch (Figure 3B-ii) and results were similar to curcumin-treated cells (Figure 3B-iii).

A decrease in both TNF- α and IL-6 (~2.5 fold) level was observed at the early and late passages (Figure 3B-iv and v) as compared to the control. Senescence-like cells were observed at the LP as compared to the EP (Figure 4B). Furthermore, collagen deposition was quantified by Sircol collagen assay at both the passages (Figure 4A-vii). An increment in the red colored hue of thicker collagen fibers was observed in the peptide (Figure 4A-ii and v) treated cells at early and late as compared to the control (Figure 4A-i and iv). This data proved the cell migration and ECM promoting the activity of the peptide.

4.7 | Attenuation of senescence-associated genes' expression

To examine the senescence-like morphological and functional changes, SA-β-G activity (a cellular senescence marker) was determined at the early and late passages (Figure 4B-i to vi). Senescence-related changes were observed in the control at aging as shown in Figure 4B-i. The percentage of SA-β-gal-positive cells were noted to be significantly ($P < 0.01$) lower in the peptide and curcumin-treated group as compared to the nontreated group (Figure 4B-vii). To further prove the senescence-like changes in the fibroblasts, a well-accepted marker of senescence, p21 (Figure 4B-viii) and p16 (Figure 4B-ix) were analyzed by qPCR. The expressions of both the markers were significantly more (nearly two-fold) in late passaged fibroblasts indicating senescence state of the cells. Both p21 and p16 were found to be significantly

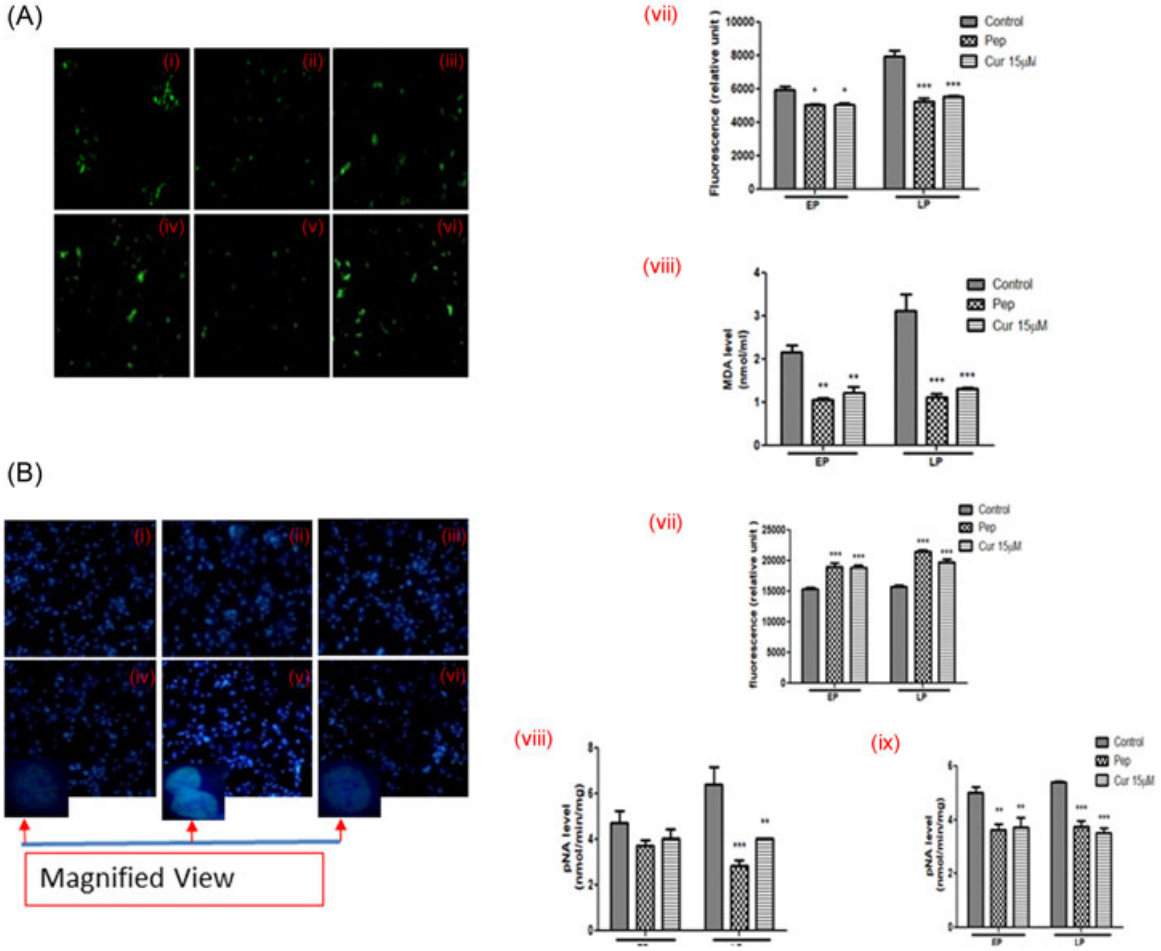

FIGURE 2 A, Effect of the peptide on NO and MDA production in fibroblast cells. Representative fluorescent images of NO production at early passage. (i) control (ii) Peptide (iii) Curcumin 15 μM. Representative fluorescent images at late passage (iv) Control (v) Peptide (vi) Curcumin 15 μM (vii) Quantitative analysis of fluorescent intensity at both passages (viii) Level of MDA at both passages. The results are expressed as mean ± SEM for n = 3. *$P < 0.05$, **$P < 0.01$ and ***$P < 0.001$ in comparison to control. B, Effect of the peptide on DNA damage, cell proliferation and apoptosis. Representative photomicrographs of Hoechst 33258 positive cells with magnified nuclear view using fluorescent microscopy at early passage (i) Control (ii) Peptide (iii) Curcumin and at late passage (iv) Control (v) Peptide (vi) Curcumin (vii) Quantitative analysis of fluorescent intensity of Hoechst positive cells (viii) Caspase 9 activity (ix) Caspase 3 activity at both the passages. The values are expressed as mean ± SEM value for n = 3, independent experiments. The bars bearing stars differ significantly from control (*$P < 0.05$, **$P < 0.01$, and ***$P < 0.001$)

($P < 0.001$) decreased in the peptide and curcumin-treated groups as compared to the control at both the passages.

4.8 | Effect of inhibitors on signaling pathways in the presence of peptide

4.8.1 | Effect on cell proliferation

Effect of the peptide (30 ng/mL) on cell proliferation was studied, in the presence of inhibitors for ERK, p38 MAPK, and Akt pathway. It was found that peptide with ERK and Akt inhibitors did not show any change in the proliferation of fibroblasts, while in case of peptide treatment with p38MAPK inhibitor (co-treatment), cell viability significantly ($P < 0.05$) increased as shown in Figure 5A.

4.8.2 | Effect of the peptide on transmigration of Nrf2

To find out the effect of the peptide on the transmigration of Nrf2 from the cytoplasm to nucleus was deliberated by immunolocalization study at the LP (Figure 5B-D). Our results revealed that peptide suppressed the level of Nrf2 in the cytoplasm (Figure 5E). In contrast, peptide promoted the nuclear transmigration of Nrf2 by p38 MAPK as shown in Figure 5F. An increase in nuclear abundance of Nrf2 at LP was observed (Figure 5F).

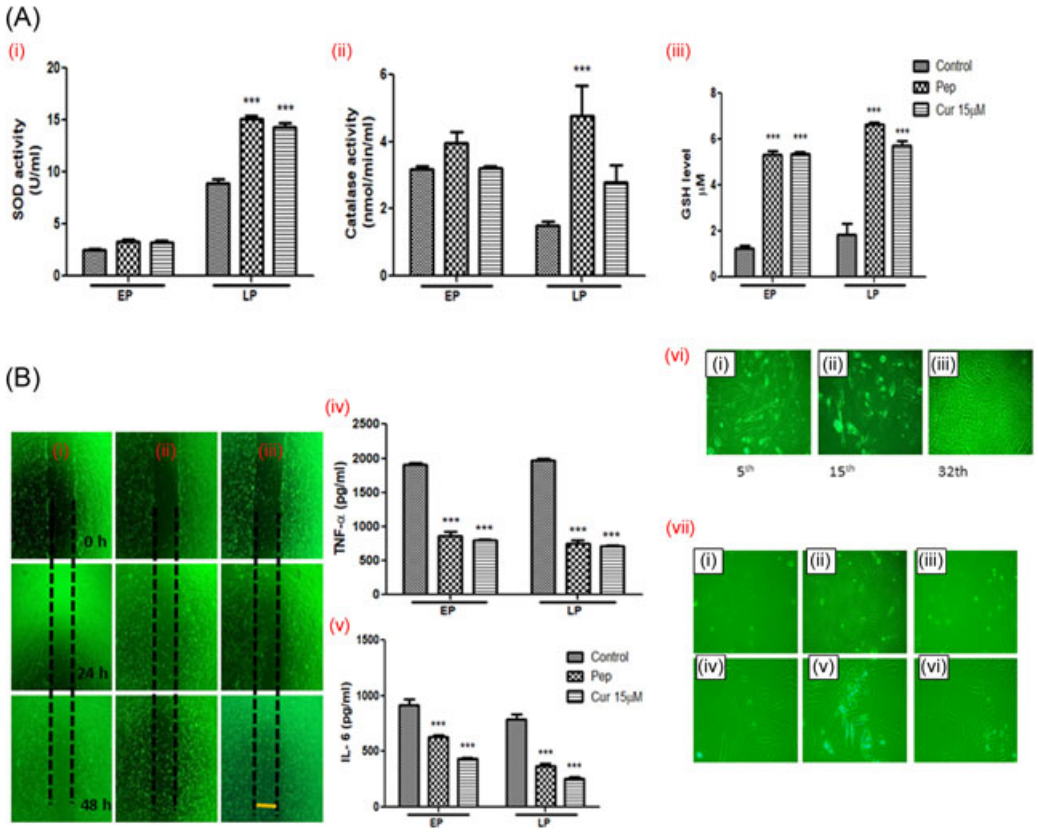

FIGURE 3 A, Effect of the peptide on SOD, Catalase activity and GSH level at early and late passaged fibroblasts. (i) SOD activity (ii) Catalase activity (iii) GSH level. The values are expressed as mean ± SEM for n = 3, independent experiments were performed. The bars bearing stars differ significantly to control (*$P < 0.05$, **$P < 0.01$, and ***$P < 0.001$). B, Effect of peptide on cell migration at late passage fibroblasts and proinflammatory cytokines secretion at early and late passages. Representative photomicrographs of cell migration (scratched area). (i) Control (ii) Peptide (iii) Curcumin 15 µM, Clear space indicated no cells after scratch. (iv) TNF-α level (v) IL-6 level. (vi) Morphological changes at early and late passages. (i) 5th passage (ii) 15th passage (iii) 32th passage. (vii) Morphological changes at 5th and 32th passages. (i) Control cells at 5th passage (ii) Peptide at 5th passage (iii) curcumin at 5th passage. (iv) control at 32th passage (v) Peptide at 32th passage (vi) curcumin at 32th passage. n = 3, independent experiments were performed

While co-treatment (Lane3) of peptide and inhibitor (SB203580), partially abolished nuclear import of Nrf2 at LP as shown in Figure 5F.

4.8.3 | The peptide downregulates the p38MAPK/NF-kB pathway in young and aged fibroblast cells

To further get insight into the molecular mechanism, protein level of p38α, phosphorylated p38MAPK, Nrf2 (NE and CE), NF (p65)-kB (NE and CE), Bcl-xL, and Bax was determined by Western blot analysis. Reduction in the protein level of NF (p65)-kB was noticed in both cytosolic and nuclear extracts (Figure 6A and 6B). Likewise decrease in proapoptotic protein (Bax) level, whereas the increase in antiapoptotic protein (Bcl-$_X$L) was observed at both the passages in the presence of the peptide (Figure 6C and 6D). In the Western blot analysis, peptide treatment (Lane2) for 24 hours significantly decreased the phospho-p38MAPK level in the cytoplasm (Figure 7D). These results are also consistent with the immunolocalization (Figure 7A-C).

5 | DISCUSSION

The aim of the present study was to investigate the mechanism of antiaging effect of milk-derived novel bioactive peptide (VLPVPQK) in aged fibroblast cells. According to the free radical theory of aging,[32] aging and its accompanying chronic diseases are attributed to the deleterious effect of free radicals on antioxidative defense system and can be countered by antioxidants that induced Nrf2 associated network of internal defense proteins.[33] Taken together, the study of antioxidant status triggered by the Nrf2 signaling pathway provides the understanding of the underlying mechanism of the novel bioactive peptide. Recently, Quan et al[4] reported that fibroblasts had distorted morphology and show senescence-associated secretory phenotype due to an imbalance in the oxidant-antioxidant homeostasis

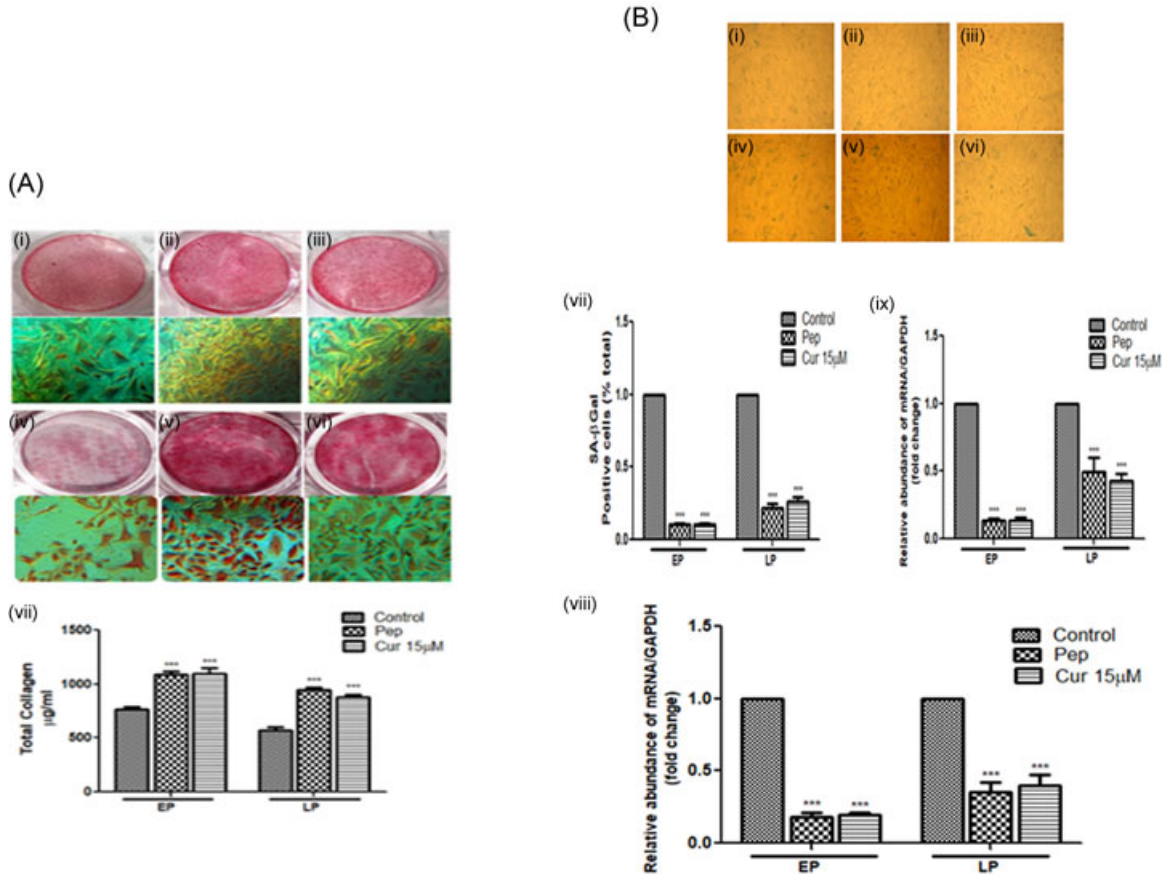

FIGURE 4 A, Effect of peptide on collagen deposition at early and late passaged fibroblasts. Effect of the peptide on collagen synthesis at early passage (i) Control (ii) Peptide (iii) Curcumin 15 μM. Effect of the peptide on collagen synthesis at late passage. (iv) Control (v) Peptide (vi) Curcumin 15 μM (vii) Quantification of collagen by extraction of Sirius red dye. The values are expressed as mean ± SEM value for n = 3, independent experiments. The bars bearing stars differ significantly (***$P < 0.001$). B, Effect of the peptide on Senescence associated (SA-β Galactosidase) activity and aging markers (CDK inhibitors). Effect of the peptide on Senescence associated (SA-β Galactosidase) activity at early passage (i) Control (ii) Peptide (iii) Curcumin 15 μM. Effect of the peptide on Senescence associated (SA-β Galactosidase) activity at late passage (iv) Control (v) Peptide (vi) Curcumin 15μM (vii) Results are presented as the percent of SA-β-Gal stained cells. (viii) Relative expression level of aging markers, p21 (ix) Relative expression level of aging markers, p16. Mean ± SEM, value for n = 3, independent experiments. The bars bearing stars differ significantly (*$P < 0.05$, **$P < 0.01$, and ***$P < 0.001$)

at aging. Likewise, studies reported in the osteoblast cells that antioxidative and osteogenic effect of bioactive peptide augmented antioxidative enzymatic system, decreased lipid peroxidation (MDA) level and partially suppressed the caspase-9/-3 in the central pathway of apoptosis.[21,34] Growth of fibroblast in presence of different concentration of the peptide showed that 30 ng/mL concentration of the peptide enhanced the cell survival rate at both early and late passages. The peptide treatment restored the flattened morphology and young intact state of fibroblasts through significantly elevating the antioxidative enzymatic and nonenzymatic proteins (SOD, CAT, and GSH) and, reducing the production of cellular oxidants (ROS, NO, and MDA) and found to be comparable to the standard natural antioxidative compound, curcumin at LP (natural aging). This suggests that peptide delayed the aging process in fibroblasts through strengthening the cellular antioxidative defense. A previous study documented that antioxidative status regulated by Nrf2, transcription factor (master regulator) in a coordinated manner through Nrf2-ARE (antioxidative response element) interaction. This triggered the expression of a panel of antioxidant enzymes in PC 12 cells.[14] Moreover, a decrease in the nuclear level of Nrf2 with age has been reported in mice astrocytes and rat livers.[35-37] To address the antiaging effect of the peptide via restoring antioxidative system through Nrf2 signaling, many proteins of the pathway were analyzed. Nuclear transmigration and transcription activity of Nrf2 is induced by p38MAP kinases.[14] p38MAP kinases are a class of MAPK that are activated in response to increasing in ROS, apoptotic caspases, stress stimuli such as pro-inflammatory cytokines (TNF-α, IL-6) and redox imbalance due to up-regulated p21 and p16. Both p21 and p16 are cyclin-dependent kinase inhibitor and are very important causative factor for

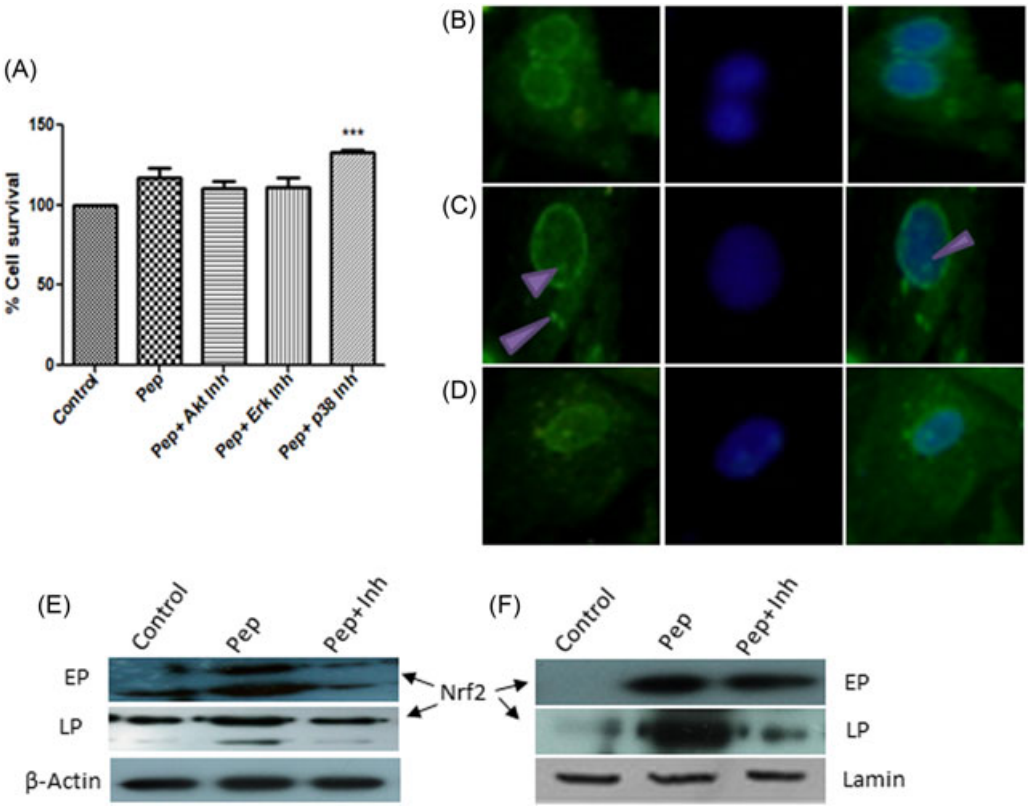

FIGURE 5 To delineate the downstream signaling. A, MTT assay at early passage. Nrf2 level after Peptide treatment was examined in the fibroblasts cell culture. Immunolocalization of Nrf2 protein at late passage fibroblasts (B) Control (C) Peptide (D) Co-treatment. After treatment, isolated proteins were subjected to western blotting analysis (E) Nrf2 cytoplasmic extract (F) Nrf2 nucleus extract. The values are expressed as mean ± SEM value for n = 3, independent experiments. The bars bearing stars differ significantly to control (***$P < 0.001$)

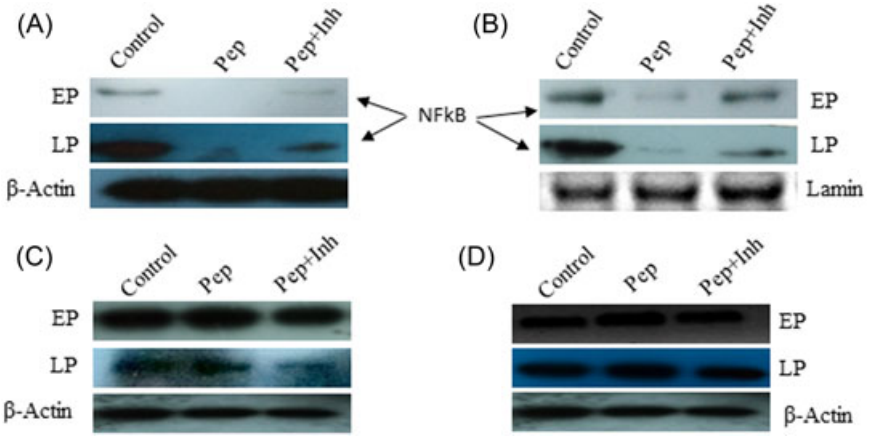

FIGURE 6 Effect of the peptide treatment on NF-κB signaling in fibroblast cells. After treatment, protein samples (50 μg) were subjected to western blotting (A) NFkB (P65) cytosolic extract (B) NFkB (P65) nucleic extract. Pro-apoptotic (Bax) and anti-apoptotic marker (Bcl-xL) were analyzed, (C) Bax protein (D) Bcl-xL protein. β-Actin served as the endogenous housekeeping protein. The values are expressed as mean ± SEM value for n = 3, independent experiments. The bars bearing stars differ significantly to control (**$P < 0.01$, and ***$P < 0.001$)

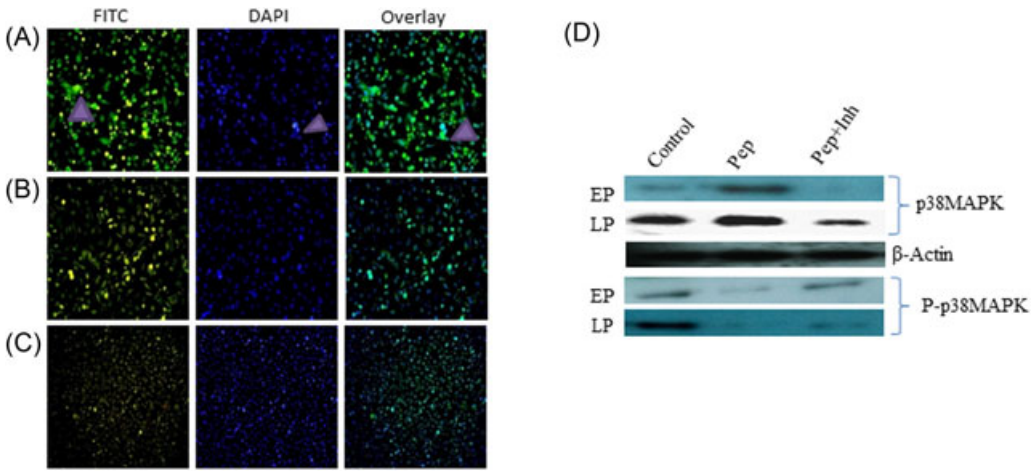

FIGURE 7 Effect of the peptide on p38 MAPK signaling. Immunolocalization of Phospho-p38MAPK (A) control (B) peptide (C) co-treatment at late passaged fibroblast cells. (D) Western blot results of p38 and Phospho- p38MAPK

senescent associated cell-cycle arrest.[38-41] The study showed that the peptide reduced the level of phosphorylated p38MAP kinases in cytoplasm to inhibit NF-kB activation and, facilitated the activation of the inactive Nrf2 for nuclear transmigration. However, a reduction in p21 and p16 apoptotic proteins was also observed in aged fibroblasts. To further explore the antiaging effect of the peptide, cellular DNA damage and caspase activity was measured. Previous studies suggested that age-associated mitochondrial damage activates caspase-9, which further induces apoptosis by downstream activation of caspase-3 and ultimately, causing DNA fragmentation and apoptosis in aged dermal fibroblasts.[4,42-44] The present study revealed that the peptide treatment significantly reduced the activities of caspase-9/-3, reversed the growth arrest and concurrently, maintained the nuclear integrity, and division in aged fibroblast cells. Senescent cells express a specific type of SA-β-gal enzyme. It is one of the most commonly used markers of cell aging.[4,30,35,45] Quan and colleagues reported that percentage of SA-β-gal positive cells increased in natural aging and in photo-aging conditions. Similarly, the number of SA-β-gal positive cells increased significantly in LP than EP in the

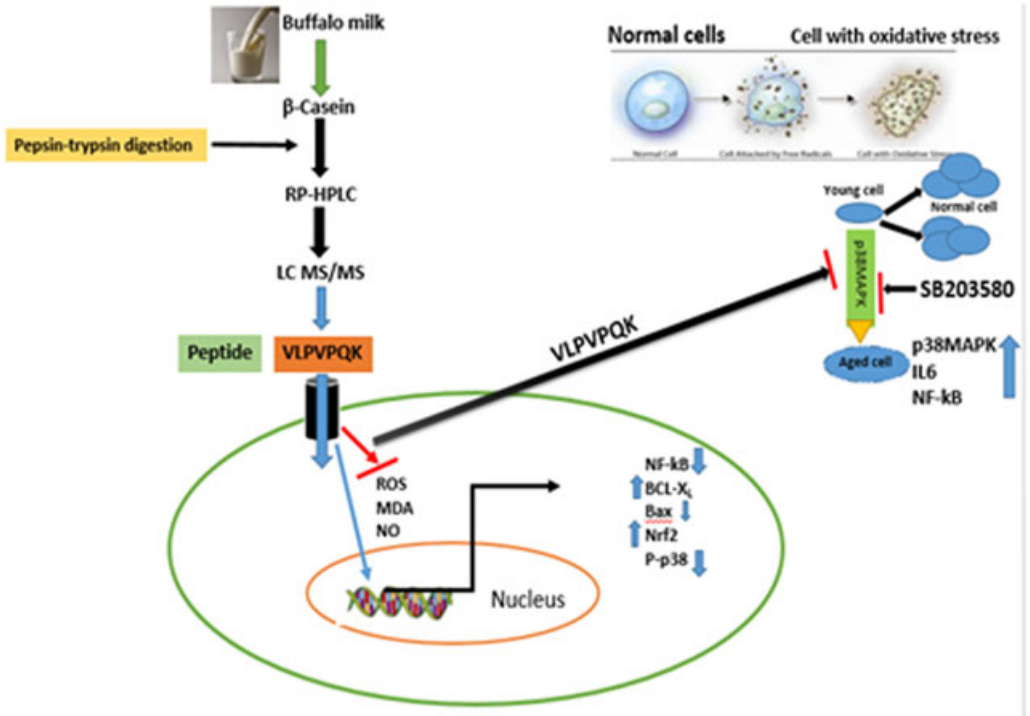

FIGURE 8 Schematic mechanism of milk-derived bioactive peptide to rejuvenate aged fibroblast cells

present investigation. But, the peptide treatment tremendously decreased SA-β-gal stained cells in aging. Moreover, in line with earlier studies where it has been reported that p38 MAPK delayed wound healing due to enhanced collagen fibril fragmentation and, reduced the spreading of cells by pro-inflammatory cytokines, that is, TNF-α, IL-6 during aging,[4,35,46] the present study too showed that fibroblasts without peptide (control) showed less wound healing due to higher amount of pro-inflammatory cytokines but the peptide treatment caused enhancement in the rate of wound healing due to reduction in pro-inflammatory cytokines in fibroblasts in the presence of peptide. In addition, Chung et al[47] showed that antiaging action of curcumin is arbitrated via inhibiting NF-kB transcription activation and suggested its potential contribution to the reduced level of pro-inflammatory cytokines, particularly TNF-α. So, to establish the role of NF-kB signaling in antiaging effect of peptide, total collagen content, cell migration, TNF- α, and IL-6 levels were measured. The peptide treatment significantly reduced the nuclear and cytosolic NF-kB level in aged fibroblasts. In the present study, it was found that peptide enhanced thick collagen fibers growth and maintained uniform cell migration by decreasing TNF-α and IL-6 level in aged fibroblasts. Moreover, apoptosis is associated with aging and therefore, to understand the possible antiapoptotic role of peptide, expression of key markers, Bcl-xL, and Bax in Nrf2 signaling was analyzed. The culturing of fibroblasts in presence of peptide caused elevation in antiapoptotic, Bcl-xL expression, while diminution in proapoptotic, Bax protein. These results suggest that peptide protected the aged fibroblast cells by downregulating apoptosis-like death signals, improving collagen synthesis, restoring phenotypic changes, and decreasing inflammatory cytokines through the down-regulation of NF-kB/p38MAP kinase pathway via activation of Nrf2, transcription factor.

6 | CONCLUSION

Our study suggests that novel milk derived antioxidative peptide (VLPVPQK) has antiageing effect. It enhanced cellular antioxidative defense system, which is mediated by the activation of Nrf2 transcription factor and down-regulation of NF-kB/p38MAP kinase pathway in aged fibroblast cells (Figure 8). This study provides the first evidence of milk-derived bioactive peptide for antiaging activity. In future, it would be interesting to further validate the use of peptide as an antiaging agent.

ACKNOWLEDGMENT

The authors are grateful to the Director, ICAR-National Dairy Research Institute (Letter No. 1(4)/2016-17/AB), Karnal for providing funding and laboratory facilities to carry out this piece of work. The author KN also acknowledges CSIR-UGC-MHRD (309309), India for providing JRF fellowship and all other financial assistance.

CONFLICTS OF INTEREST

The authors declare that they have no conflicts of interest.

AUTHOR CONTRIBUTIONS

The experiments were conceived and designed by KS, KN, and RS; performed by: KN, DS, and MBS; the data were analyzed by KN and RS; reagents/materials were contributed by KR; and the paper was written by KN.

ORCID

Suman Kapila http://orcid.org/0000-0003-2627-773X

REFERENCES

1. Hayflick L, Moorhead PS. The serial cultivation of human diploid cell strains. *Exp Cell Res*. 1961;25:585-621. https://doi.org/10.1016/0014-4827 (61)90192-6
2. Campisi J. Replicative senescence: an old lives' tale? *Cell*. 1996;84:497-500. https://doi.org/10.1016/S0092-8674 (00)81023-5
3. Campisi J, Kim S, Lim CS, Rubio M. Cellular senescence, cancer and aging: the telomere connection. *Exp Gerontol*. 2001;36:1619-1637. https://doi.org/10.1016/S0531-5565 (01)00160-7
4. Quan C, Cho MK, Perry D, Quan T. Age-associated reduction of cell spreading induces mitochondrial DNA common deletion by oxidative stress in human skin dermal fibroblasts: implication for human skin connective tissue aging. *J Biomed Sci*. 2015b;22:62. https://doi.org/10.1186/s12929-015-0167-6
5. Quan T. Skin connective tissue aging and dermal fibroblasts. *Dermal Fibroblasts: Histological Perspectives, Characterization and Role in Disease*. Hauppauge, NY: Nova Science Publishers, Inc; 2013. Chapter 3.31–56.
6. Quan T, Fisher GJ. Role of age-associated alterations of the dermal extracellular matrix microenvironment in human skin aging: a mini-review. *Gerontology*. 2015a;61(5):427-434. https://doi.org/10.1159/000371708
7. Quan T, Shao Y, He T, Voorhees JJ, Fisher GJ. Reduced expression of connective tissue growth factor (CTGF/CCN2) mediates collagen loss in chronologically aged human skin. *J Invest Dermatol*. 2010;130(2):415-424. https://doi.org/10.1038/jid.2009.224
8. Selokar NL, Saini M, Muzaffer M, et al. Roscovitine treatment improves synchronization of donor cell cycle in G0/G1 stage and in vitro development of handmade cloned buffalo (Babalus bubalis) embryos. *Cell Reprogram*. 2012;14:146-154. https://doi.org/10.1089/cell.2011.0076
9. Molnár Á, Theodoras AM, Zon LI, Kyriakis JM. Cdc42Hs, but not Rac1, inhibits serum-stimulated cell cycle progression at G1/S through a mechanism requiring p38/RK. *J Biol Chem*. 1997;272:13229-13335. https://doi.org/10.1074/jbc.272.20.13229

10. Yee AS, Paulson EK, McDevitt MA, et al. The HBP1 transcriptional repressor and the p38 MAP kinase: unlikely partners in G1 regulation and tumor suppression. *Gene*. 2004;336:1-13. https://doi.org/10.1016/j.gene.2004.04.004
11. Henkart PA. ICE family proteases: mediators of all apoptotic cell death? *Immunity*. 1996;4(3):195-201. https://doi.org/org/10.1016/S1074-7613 (00)80428-8
12. Huang S, Jiang Y, Li Z, et al. Apoptosis signaling pathway in T cells is composed of ICE/Ced-3 family proteases and MAP kinase kinase 6β. *Immunity*. 1997;6:739-749. https://doi.org/org/10.1016/S1074-7613 (00)80449 5
13. Rubin H. The disparity between human cell senescence in vitro and lifelong replication in vivo. *Nat Biotechnol*. 2002;20:675-681. https://doi.org/10.1038/nbt0702-675
14. Minelli A, Conte C, Grottelli S, Bellezza M, Cacciatore I, Bolaños JP. Cyclo (His-Pro) promotes cytoprotection by activating Nrf2-mediated up-regulation of antioxidant defence. *J Cell Mol Med*. 2009;13(6):1149-1161. https://doi.org/10.1111/j.1582-4934.2008.00326.x
15. Kumar R, Singhal V, Sangwan RB, Mann B. Comparative studies on antioxidant activity of buffalo and cow milk casein and their hydrolysates. *Milchwissenschaft*. 2010;65:287-290.
16. Praveesh BV, Angayarkanni J, Palaniswamy M. Antihypertensive and anticancer effect of cow milk fermented by lactobacillus plantarum and lactobacillus casei. *Inter J Pharm Pharma Sciences*. 2011;3(Suppl 5):452-456.
17. Shanmugam VP, Kapila S, Sonfack TK, Kapila R. Antioxidative peptide derived from enzymatic digestion of buffalo casein. *Inter Dairy J*. 2015;42:1-5. https://doi.org/org/10.1016/j.idairyj.2014.11.001
18. Reddi S, Kumar N, Vij R, Mada SB, Kapila S, Kapila R. Akt drives buffalo casein-derived novel peptide-mediated osteoblast differentiation. *J Nutr Biochem*. 2016a;38:134-144. https://doi.org/10.1016/j.jnutbio.2016.08.003
19. Reddi S, Shanmugam VP, Kapila S, Kapila R. Identification of buffalo casein derived bioactive peptides with osteoblast proliferation activity. *Eur Food Res Technol*. 2016b;242:2139-2146. https://doi.org/10.1007/s00217-016-2710-4
20. Reddi S, Shanmugam VP, Tanedjeu KS, Kapila S, Kapila R. Effect of buffalo casein derived novel bioactive peptides on osteoblast differentiation. *Eur J Nutr*. 2016c;57:593-605. https://doi.org/10.1007/s00394-016-1346-2
21. Mada S, Reddi S, Kumar N, Kapila S, Kapila R. Protective effects of casein-derived peptide VLPVPQK against hydrogen peroxide-induced dysfunction and cellular oxidative damage in rat osteoblastic cells. *Hum Exp Toxicol*. 2016;36:1-14. https://doi.org/10.1177/0960327116678293
22. Vij R, Reddi S, Kapila S, Kapila R. Transepithelial transport of milk derived bioactive peptides VLPVPQK. *Food Chem*. 2016;190:681-688. https://doi.org/10.1016/j.foodchem.2015.05.121
23. Wang H, Van Blitterswijk CA, Bertrand-De Haas M, Schuurman AH, Lamme EN. Improved enzymatic isolation of fibroblasts for the creation of autologous skin substitutes. *In Vitro Cell Dev Biol Anim*. 2004;40:268-277. https://doi.org/10.1290/0408055.1
24. Priya D, Selokar N, Raja A, et al. Production of wild buffalo (Bubalus arnee) embryos by interspecies somatic cell nuclear transfer using domestic buffalo (*Bubalus bubalis*) oocytes. *Reprod Domest Anim*. 2014;49(2):343-351. https://doi.org/10.1111/rda.12284
25. Abe K, Saito H. Characterization of t-Butyl hydroperoxide toxicity in cultured rat cortical neurons and astrocytes. *Pharmacol Toxicol*. 1998;83:40-46.
26. Lima CF, Pereira-Wilson C, Rattan SIS. Curcumin induces heme oxygenase-1 in normal human skin fibroblasts through redox signaling: relevance for anti-aging intervention. *Mol Nutr Food Res*. 2011;55:430-442. https://doi.org/10.1002/mnfr.201000221
27. Singh S, Aggarwal BB. Activation of transcription factor NF-κB is suppressed by curcumin (diferuloylmethane). *J Biol Chem*. 1995;270(42):24995-25000.
28. Liang CC, Park AY, Guan JL. In vitro scratch assay: a convenient and inexpensive method for analysis of cell migration in vitro. *Nat Protoc*. 2007;2:329-333. https://doi.org/10.1038/nprot.2007.30
29. Anderson SML, Elliott RJ. Evaluation of a new, rapid collagen assay. *Biochem Soc Trans*. 1991;19:389s-389S. https://doi.org/10.1042/bst019389s
30. Dimri GP, Lee X, Basile G, et al. A biomarker that identifies senescent human cells in culture and in aging skin in vivo. *Proc Natl Acad Sci USA*. 1995;92:9363-9367.
31. Lowry OH, Rosebrough NJ, Farr AL, Randall RJ. Protein measurement with the folin phenol reagent. *J Biol Chem*. 1951;193:265-275.
32. Harman D. Aging: a theory based on free radical and radiation chemistry. *J Gerontol*. 1956;11:298-300.
33. Volonte D, Liu Z, Musille PM, et al. Inhibition of nuclear factor erythroid 2–related factor (Nrf2) by caveolin-1 promotes stress induced premature senescence. *Mol Biol Cell*. 2013;24(12):1852-1862. https://doi.org/10.1091/mbc.E12-09-0666
34. Devi S, Kumar N, Kapila S, et al. Buffalo casein derived peptide can alleviates H_2O_2 induced cellular damage and necrosis in fibroblast cells. *Exp Toxico Pathol*. 2017;69:485-495. https://doi.org/10.1016/j.etp.2017.04.009
35. Duan W, Zhang R, Guo Y, et al. Nrf2 activity is lost in the spinal cord and its astrocytes of aged mice. *In Vitro Cell Dev Biol Anim*. 2009;45:388-397. https://doi.org/10.1007/s11626-009-9194-5
36. Shih PH, Yen GC. Differential expressions of antioxidant status in aging rats: the role of transcriptional factor Nrf2 and MAPK signaling pathway. *Biogerontology*. 2007;8:71-80. https://doi.org/10.1007/s10522-006-9033-y
37. Suh JH, Shenvi SV, Dixon BM, et al. Decline in transcriptional activity of Nrf2 causes age-related loss of glutathione synthesis, which is reversible with lipoic acid. *Proc Natl Acad Sci USA*. 2004;101:3381-3386. https://doi.org/10.1073/pnas.0400282101
38. Ito K, Hirao A, Arai F, et al. Reactive oxygen species act through p38 MAPK to limit the lifespan of hematopoietic stem cells. *Nat Med*. 2006;12:446-451. https://doi.org/10.1038/nm1388
39. Li Z, Li J, Bu X, et al. Age-induced augmentation of p38 MAPK phosphorylation in mouse lung. *Exp Gerontology*. 2011;46:694-702. https://doi.org/10.1016/j.exger.2011.04.005
40. Liu J, Finkel T. Stem cell aging: what bleach can teach. *Nat Med*. 2006;12:383-384. https://doi.org/10.1038/nm0406-383
41. Davis T, Baird DM, Haughton MF, Jones CJ, Kipling D. Prevention of accelerated cell aging in Werner syndrome using a p38 mitogen-activated protein kinase inhibitor. *J Gerontol A Biol Sci Med Sci*. 2005;60:1386-1393.

42. Zhang J, Patel JM, Block ER. Enhanced apoptosis in prolonged cultures of senescent porcine pulmonary artery endothelial cells. *Mech Ageing Dev*. 2002a;123:613-625. https://doi.org/org/10.1016/S0047-6374 (01)00412-2
43. Zhang Y, Chong E, Herman B. Age-associated increases in the activity of multiple caspases in Fisher 344 rat organs. *Exp. Gerontology*. 2002b;37:777-789. https://doi.org/org/10.1016/S0531-5565 (02)00013-X
44. Cohen GM. Caspases: the executioners of apoptosis. *Biochem J*. 1997;326:1-16.
45. Lawless C, Wang C, Jurk D, Merz A, Zglinicki T, Passos JF. Quantitative assessment of markers for cell senescence. *Exp Gerontology*. 2010;45:772-778. https://doi.org/10.1016/j.exger.2010.01.018
46. Ballas CB, Davidson JM. Delayed wound healing in aged rats is associated with increased collagen gel remodelling and contraction by skin fibroblasts, not with differences in apoptotic or myofibroblast cell populations. *Wound Repair Regen*. 2001;9:223-237. https://doi.org/10.1046/j.1524-475x.2001.00223.x
47. Chung S, Yao H, Caito S, Hwang J, Arunachalam G, Rahman I. Regulation of SIRT1 in cellular functions: role of polyphenols. *Arch Biochem Biophys*. 2010;501:79-90. https://doi.org/10.1016/j.abb.2010.05.003

SUPPORTING INFORMATION

Additional supporting information may be found online in the Supporting Information section at the end of the article.

How to cite this article: Kumar N, Reddi S, Devi S, Mada SB, Kapila R, Kapila S. Nrf2 dependent antiaging effect of milk-derived bioactive peptide in old fibroblasts. *J Cell Biochem*. 2018;1-15. https://doi.org/10.1002/jcb.28246